C. T.-C. Nguyen, “Micromechanical circuits for communications,” *Proceedings*, 2000 International Conference on Conference on High Density Interconnect and Systems Packaging, Denver, Colorado, April 25-28, 2000, pp. 112-117.

Micromechanical Circuits for Communications

Clark T.-C. Nguyen

Center for Integrated Microsystems
Department of Electrical Engineering and Computer Science
University of Michigan
Ann Arbor, Michigan 48109-2122
Tel: (734)764-1220, FAX: (734)763-9324, email: ctnguyen@eecs.umich.edu

Abstract

Micromechanical communication circuits fabricated via IC-compatible MEMS technologies and capable of low-loss filtering, mixing, switching, and frequency generation, are described with the intent to miniaturize wireless transceivers. A possible transceiver front-end architecture is then presented that uses these micromechanical circuits in large quantities to substantially reduce power consumption. Technologies that integrate MEMS and transistor circuits into single-chip systems are then reviewed with an eye towards the possibility of single-chip communication transceivers.

Keywords: MEMS, resonator, filter, oscillator, transceiver, switch

I. Introduction

Due to their need for high frequency selectivity and low noise frequency manipulation, portable wireless communication transceivers continue to rely on off-chip resonator technologies that interface with transistor electronics at the board-level. In particular, highly selective, low loss radio frequency (RF) and intermediate frequency (IF) bandpass filters generally require SAW or quartz acoustic resonator technologies with Q's in excess of 1,000. In addition, LC resonator tanks with Q's greater than 40 are required by voltage-controlled oscillators (VCO's) to achieve sufficiently low phase noise. These off-chip resonator components then contribute to the substantial percentage (often up to 80%) of portable transceiver area taken up by board-level, passive components.

Recent advances in IC-compatible microelectromechanical system (MEMS) technologies that make possible micro-scale, mechanical circuits capable of low-loss filtering, mixing, switching, and frequency generation, now suggest methods for boardless integration of wireless transceiver components. In fact, given the existence already of technologies that merge micromechanics with transistor circuits onto single silicon chips [1], single-chip transceivers may eventually be possible, perhaps using alternative architectures that maximize the use of passive, high-Q, micromechanical circuits to reduce power consumption for portable applications.

This paper presents an overview of the micromechanical circuits and associated technologies expected to play key roles in reducing the size and power consumption of future communication transceivers.

II. Micromechanical Circuits

Although mechanical circuits, such as quartz crystal resonators and SAW filters, provide essential functions in the majority of transceiver designs, their numbers are generally suppressed due to their large size and finite cost. Unfortunately, when minimizing the use of high-Q components, designers often trade power for selectivity (i.e., Q), and hence, sacrifice transceiver performance.

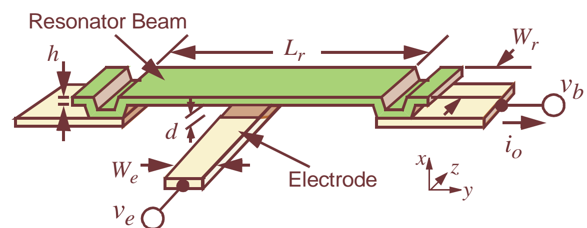

Fig. 1: Perspective-view schematic of a clamped-clamped beam μmechanical resonator in a general bias and excitation configuration.

By shrinking dimensions and introducing batch fabrication techniques, MEMS technology provides a means for relaxing the present constraints on the complexity of mechanical circuits, with implications not unlike those that integrated circuit technology had on transistor circuit complexity. Before exploring the implications, specific μmechanical circuits are first reviewed.

A. Micromechanical Beam Element

To date, the majority of μmechanical circuits most useful for communication applications have been realized using simple μmechanical flexural-mode beam elements, such as shown in Fig. 1 with clamped-clamped boundary conditions. Although several micromachining technologies are available to realize such an element in a variety of different materials, surface micromachining has been the preferred method for μmechanical communication circuits, mainly due to its flexibility in providing a variety of beam end conditions and electrode locations, and its ability to realize very complex geometries with multiple levels of suspension.

Figure 2 summarizes the essential elements of a typical surface-micromachining process that produces a clamped-clamped beam. In this process, a series of film depositions and lithographic patterning steps—identical to similar steps used in planar IC fabrication technologies—are utilized to first achieve the cross-section shown in Fig. 2(a). Here, a

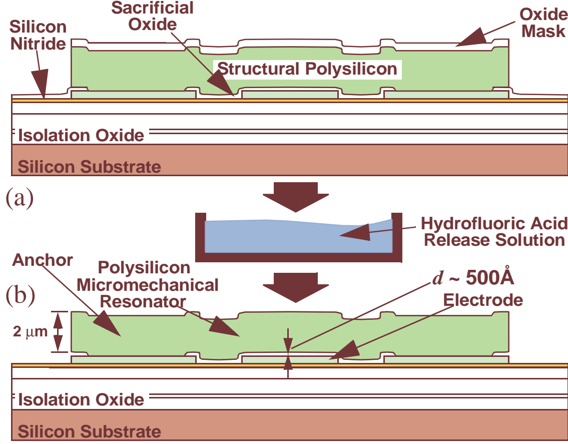

Fig. 2: Cross-sections describing surface micromachining. (a) Required film layers up to the release etch step. (b) Resulting free-standing beam following a release etch in hydrofluoric acid.

sacrificial oxide layer supports the structural polysilicon material during deposition, patterning, and subsequent annealing. In the final step of the process, the wafer containing cross-sections similar to Fig. 2(a) is dipped into a solution of hydrofluoric acid, which etches away the sacrificial oxide layer without significantly attacking the polysilicon structural material. This leaves the free-standing structure shown in Fig. 2(b), capable of movement in three dimensions, if necessary, and more importantly, capable of vibrating with high Q and good temperature stability, with temperature coefficients on the order of -10 ppm/^{o}C [2].

For frequency reference, filtering, and mixing applications, the resonance frequency of this flexural-mode mechanical beam is of great interest. For the clamped-clamped beam of Fig. 1, the expression for resonance frequency can be written as (ignoring stress) [3]

$$f_o = \frac{1}{2\pi}\sqrt{\frac{k_r}{m_r}} = 1.03\kappa\sqrt{\frac{E}{\rho}}\frac{h}{L_r^2}(1-g(V_P))^{1/2}, \qquad (1)$$

where E and ρ are the Young's modulus and density of the structural material, respectively; h and L_r are specified in Fig. 1; and κ is a scaling factor that models the effects of surface topography in actual implementations [3]. From (1), geometry clearly plays a major role in setting the resonance frequency, and in practice, attaining a specified frequency amounts to CAD layout of the proper dimensions. Table I presents expected resonance frequencies for various beam dimensions, modes, and structural materials, showing a wide range of attainable frequencies, from VHF to UHF.

To complete the mechanical circuit element, input and output ports are required. These can be either electrical or mechanical, and in any number. In Fig. 1, two electrical inputs are shown, v_e and v_b, applied to the electrode and beam, respectively. In this configuration, the difference voltage (v_e–v_b) is effectively applied across the electrode-to-resonator capacitor gap, generating a force between the stationary electrode and movable beam given by

Table I: μMechanical Resonator Frequency Design*

Freq. [MHz]	Material	Mode	h_r [μm]	W_r [μm]	L_r [μm]
70	silicon	1	2	8	15.18
110	silicon	1	2	8	11.86
250	silicon	1	2	4	7.34
870	silicon	2	4	4	7.13
870	diamond	1	4	4	6.47
1800	silicon	2	4	8	4.98
1800	diamond	2	4	4	7.58

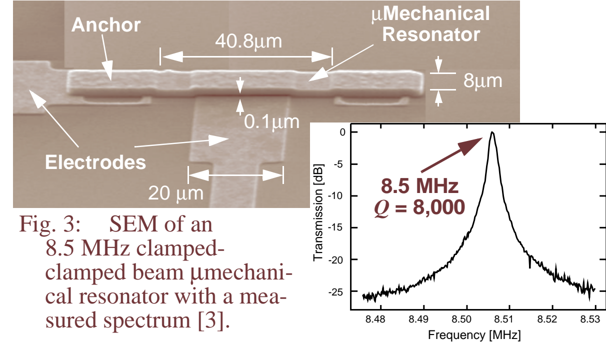

Fig. 3: SEM of an 8.5 MHz clamped-clamped beam μmechanical resonator with a measured spectrum [3].

$$F_d = -\frac{\partial E}{\partial x} = -\frac{1}{2}(v_e - v_b)^2\frac{\partial C}{\partial x}, \qquad (2)$$

where x is displacement (with direction indicated in Fig. 1), and ($\partial C/\partial x$) is the change in resonator-to-electrode capacitance per unit displacement.

B. HF Micromechanical Reference Tank.

The high Q and thermal stability of the resonance frequency of single μmechanical beam elements make them good candidates for tanks in reference oscillator applications. When using the resonator as a tank or filter circuit (as opposed to a mixer, to be discussed later), a dc-bias voltage V_P is applied to the conductive beam, while an ac excitation signal v_i=$V_i\cos\omega_i t$ is applied to the underlying electrode. In this configuration, a dominant force component is generated at ω_i, which drives the beam into mechanical resonance when ω_i=ω_o, creating a dc-biased (via V_P) time-varying capacitance between the electrode and resonator, and sourcing an output current i_o=$V_P(\partial C/\partial x)(\partial x/\partial t)$, as shown in Fig. 1. When plotted versus the frequency of v_i, i_o traces out a bandpass biquad characteristic with a Q~10,000 in vacuum (c.f., Fig. 3)—very suitable for reference oscillators.

C. VHF Micromechanical Reference Tank.

Although impressive at HF, the clamped-clamped beam device of Fig. 3 begins to lose a substantial fraction of its internal energy to the substrate at frequencies past 30 MHz, and this limits the attainable Q at VHF. To retain Q's around 8,000 at VHF, a beam with free-free ends is required, such as shown in Fig. 4, in which additional mechanical circuit complexity is added to allow free-free operation, and to

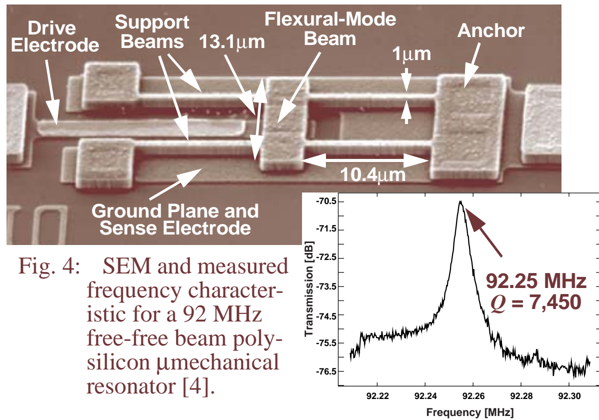

Fig. 4: SEM and measured frequency characteristic for a 92 MHz free-free beam polysilicon μmechanical resonator [4].

reduce anchor losses to the substrate [4]. Via proper support beam design, anchor losses can be greatly attenuated in this structure, and Q's on the order of 8,000 are attained even at 92 MHz.

D. Micromechanical Filters

Among the more useful μmechanical circuits for communications are those implementing low-loss bandpass filters. Figure 5(a) presents the SEM of a two-resonator 68 MHz μmechanical filter, comprised of three mechanical links interconnected in a network designed to yield the bandpass spectrum shown in Fig. 5(b). The design of this filter has been covered extensively in previous literature [3]. For the present purposes, however, the operation of this filter can be deduced from its equivalent circuit, shown in Fig. 5(c). Here, each of the outside links serve as capacitively transduced μmechanical resonators with equivalent circuits based on *LCR* networks. The connecting link actually operates as an acoustic transmission line, and thus, can be modeled by a *T*-network of energy storage elements. When combined together into the circuit of Fig. 5(c), these elements provide a more selective filtering function, with sharper roll-offs and increased stopband rejection over single resonator devices.

Note that Fig. 5 depicts a relatively simple mechanical circuit. Using more complicated interconnections with a larger number of beam elements and I/O ports, a wide variety of signal processing transfer functions can be realized, with even wider application ranges.

E. Micromechanical Mixer-Filters

As indicated by (2), the voltage-to-force transducer of Fig. 1 is nonlinear, relating input force F_d to input voltage (v_e–v_b) by a square law. When v_b=V_P (i.e., a dc voltage), this nonlinearity is suppressed, leading to a dominant force that is linear with v_e. If, however, signal inputs are applied to both v_e and v_b, a square law mixer results, that multiplies v_e and v_b, mixing these two input voltages down to a force component at their difference frequency. In particular, if an RF signal v_{RF} at frequency ω_{RF} is applied to electrode e, and a local oscillator signal v_{LO} at frequency ω_{LO} to electrode b, then these *electrical* signals are mixed down to a *force* signal at frequency ω_{IF}=(ω_{RF}–ω_{LO}). If the above transducer is used to couple into a μmechanical filter with a passband centered at ω_{IF} (c.f., Fig. 6), an effective mixer-filter device results that provides both mixing and filtering in one passive, μmechanical device. Since μmechanical circuits exhibit low-loss and consume virtually no dc power, such a device can greatly reduce the power consumption in transceivers, as will soon be seen.

F. Micromechanical Switches

The mixer-filter device described above is one example of a μmechanical circuit that harnesses nonlinear device properties to provide a useful function. Another very useful mode of operation that further utilizes the nonlinear nature of the device is the μmechanical switch. Figure 7 presents an operational schematic for a single-pole, single-throw μmechanical switch, seen to have a structure very similar to that of the previous resonator devices: a conductive beam or membrane suspended above an actuating electrode. The operation of the switch of Fig. 7 is fairly simple: To achieve the "on-state", apply a sufficiently large voltage across the beam and electrode to pull the beam down and short it (in either a dc or ac fashion) to the electrode.

In general, to minimize insertion loss, the majority of switches use metals as their structural materials. It is their metal construction that makes μmechanical switches so attractive, allowing them to achieve "on-state" insertion losses down to 0.1 dB—much lower than FET transistor counterparts, which normally exhibit ~2 dB of insertion loss. In addition to exhibiting such low insertion loss, μmechanical switches are extremely linear, with *IIP3*'s greater than 66 dBm [1], and can be designed to consume no dc power (as opposed to FET switches, which sink a finite current when activated).

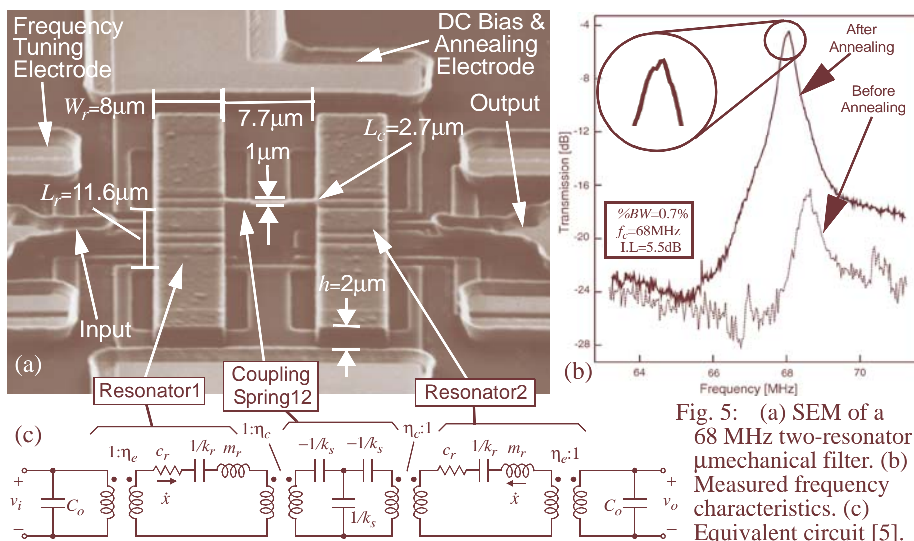

Fig. 5: (a) SEM of a 68 MHz two-resonator μmechanical filter. (b) Measured frequency characteristics. (c) Equivalent circuit [5].

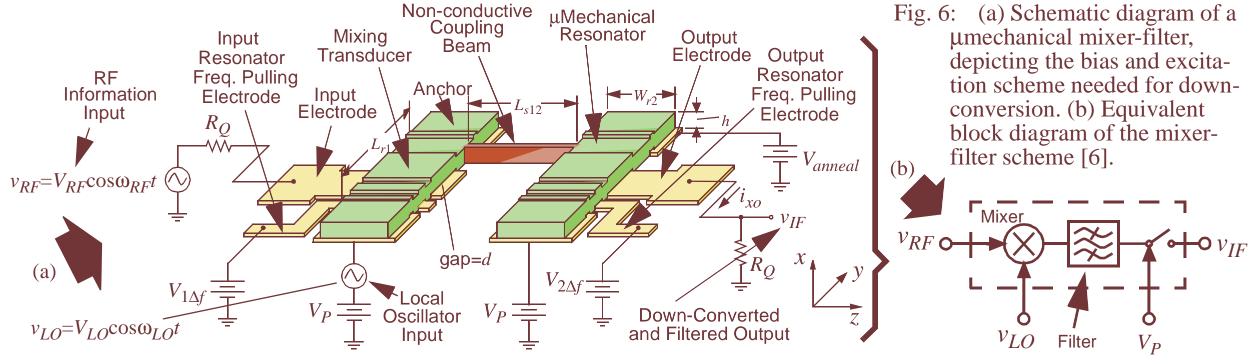

Fig. 6: (a) Schematic diagram of a µmechanical mixer-filter, depicting the bias and excitation scheme needed for down-conversion. (b) Equivalent block diagram of the mixer-filter scheme [6].

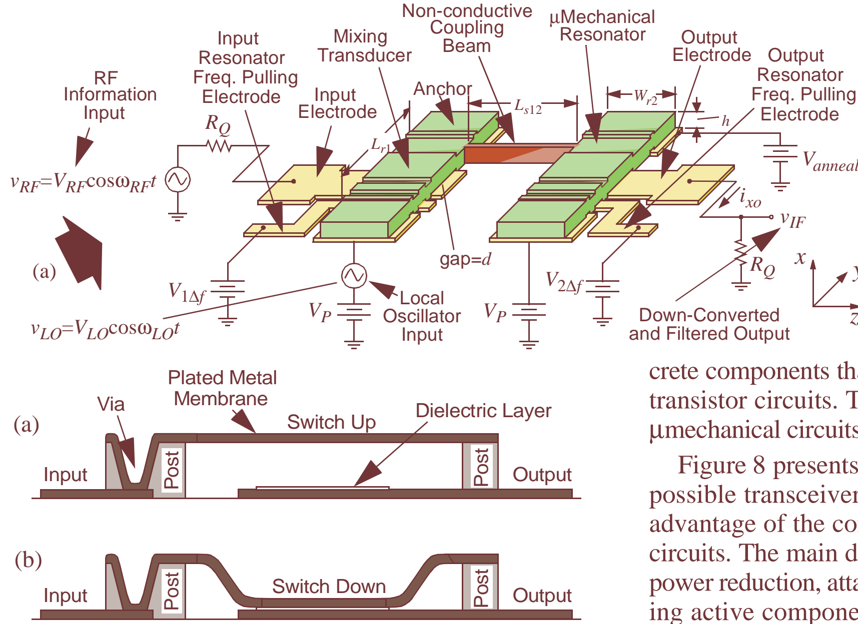

Fig. 7: Cross-sectional schematics of a typical µmechanical switch: (a) Switch up. (b) Switch down [8].

III. MEMS-Based Transceiver Architectures

Perhaps the most direct way to harness µmechanical circuits is via direct replacement of the off-chip ceramic, SAW, and crystal resonators used in RF preselect and image reject filters, IF channel-select filters, and crystal oscillator references in conventional super-heterodyne architectures. In addition, µmechanical switches can be used to replace FET T/R switches to greatly reduce wasted power in transmit mode (by as much as 280mW if the desired output power is 500mW). Furthermore, medium-Q micromachined inductors and tunable capacitors [1] can be used in VCO's and matching networks for further miniaturization.

Although beneficial, the performance gains afforded by mere direct replacement by MEMS are quite limited when compared to more aggressive uses of MEMS technology. To fully harness the advantages of µmechanical circuits, one must first recognize that due to their micro-scale size and zero dc power consumption, µmechanical circuits offer the same system complexity advantages over off-chip discrete components that planar IC circuits offer over discrete transistor circuits. Thus, to maximize performance gains, µmechanical circuits should be utilized in large numbers.

Figure 8 presents the system-level block diagram for a possible transceiver front-end architecture that takes full advantage of the complexity achievable via µmechanical circuits. The main driving force behind this architecture is power reduction, attained in several of the blocks by replacing active components by low-loss passive µmechanical ones, and by trading power for high selectivity (i.e., high-Q). Among the key performance enhancing features are: (1) an RF channel selector comprised of a bank of switchable µmechanical filters, offering multi-band reconfigurability, receive power savings via relaxed dynamic range requirements [7], and transmit power savings by allowing the use of a more efficient power amplifier; (2) use of a passive µmechanical mixer-filter to replace the active mixer normally used, with obvious power savings; (3) a VCO referenced to a switchable bank of µmechanical resonators, capable of operating without the need for locking to a lower frequency reference, hence, with orders of magnitude lower power consumption than present-day synthesizers; (4) use of a µmechanical T/R switch, with already described power savings in transmit-mode; and (5) use of µmechanical resonator and switch components around the power amplifier to enhance its efficiency.

IV. Circuits/MEMS Merging Technologies

Although a two-chip solution that combines a MEMS chip with a transistor chip can certainly be used to interface µmechanical circuits with transistor circuits, such an approach becomes less practical as the number of µme-

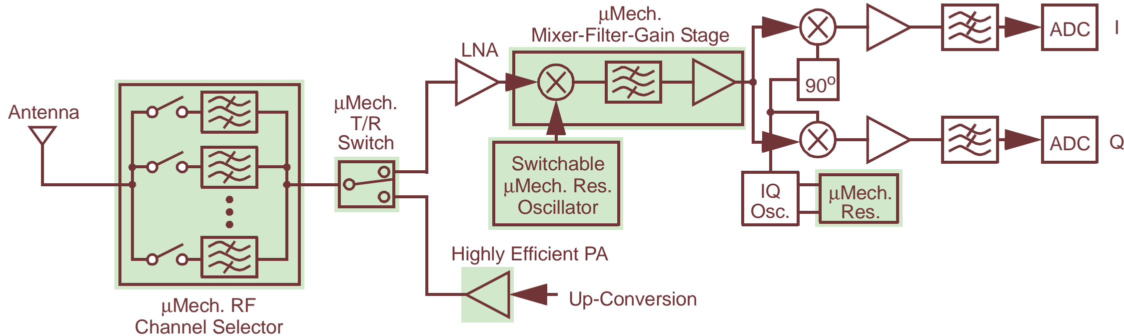

Fig. 8: System block diagram for an RF channel-select receiver architecture utilizing large numbers of micromechanical resonators in banks to trade Q for power consumption. (On-chip µmechanics are shaded.)

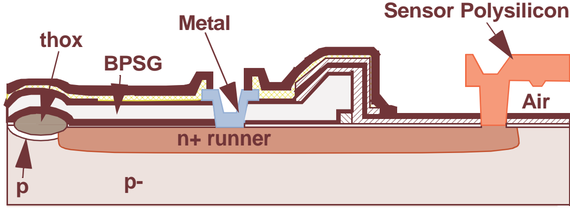

Fig. 9: Cross-section of the sensor area in Analog Devices' BiMOSII process [9].

chanical components increases. For instance, practical implementations of the switchable filter bank in Fig. 8 require multiplexing support electronics that must interconnect with each µmechanical device. If implemented using a two-chip approach, the number of chip-to-chip bonds required could become quite cumbersome, making a single-chip solution desirable.

In the pursuit of single-chip systems, several technologies that merge micromachining processes with those for integrated circuits have been developed and implemented over the past several years. These technologies can be categorized into three major approaches:

A. Mixed Circuit and Micromechanics

In the mixed circuit/micromechanics approach, steps from both the circuit and the micromachining processes are intermingled into a single process flow. Of the three approaches, this one has so far seen the most use. However, it suffers from two major drawbacks: (1) many passivation layers are required (one needed virtually every time the process switches between circuits and µmechanics); and (2) extensive re-design of the process is often necessary if one of the combined technologies changes (e.g., a more advanced circuit process is introduced). Analog Devices' BiMOSII process (Fig. 9 [9]), which has successfully produced a variety of accelerometers in large volume, is among the most successful examples of mixed circuit/ micromechanics processes.

B. Pre-Circuits

In the pre-circuits approach, micromechanics are fabricated in a first module, then circuits are fabricated in a subsequent module, and no process steps from either module are intermingled. This process has a distinct advantage over the mixed process above in that advances in each module can be accommodated by merely replacing the appropriate module. Thus, if a more advanced circuit process becomes available, the whole merging process need not be re-designed; rather, only the circuits module need be replaced. An additional advantage is that only one passivation step is required after the micromechanical module. One of the main technological hurdles in implementing this process is the large topography leftover by micromechanical processes, with features that can be as high as 9 µm, depending upon the number and geometry of structural layers. Such topographies can make photoresist spinning and patterning quite difficult, especially if submicron circuit features are desired. These problems, however, have been overcome by researchers at Sandia National Laboratories, whose *iMEMS* process (Fig. 10) performs the micromechanics module in a trench, then planarizes features using chemical mechanical polishing (CMP) before doing the circuits module [10].

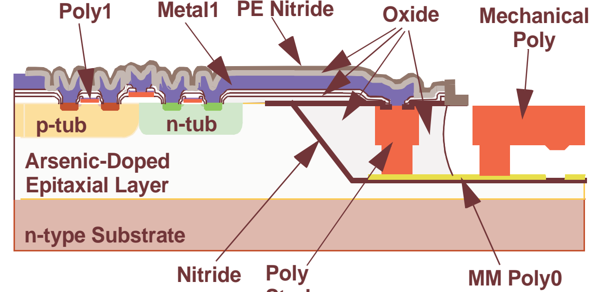

Fig. 10: Cross-section of Sandia's *iMEMS* process [10].

C. Post-Circuits

The post-circuit approach is the dual of pre-circuits, in which the circuits module comes first, followed by the micromechanics module, where again, no process steps from either module are interspersed. This process has all the advantages of pre-circuits, but with relaxed topography issues, since circuit topographies are generally much smaller than micromechanical ones. As a result, planarization is often not necessary before micromechanics processing. Post-circuit processes have the additional advantage in that they are more amenable to multi-facility processing, in which a very expensive fabrication facility (perhaps a foundry) is utilized for the circuits module, and relatively lower capital micromechanics processing is done in-house at the company site (perhaps a small start-up). Such an arrangement may be difficult to achieve with a pre-circuits process because IC foundries may not permit "dirty" micromachined wafers into their ultra-clean fabrication facilities. Post-circuit processes have taken some time to develop. The main difficulty has been that aluminum based circuit metallization technologies cannot withstand subsequent high temperature processing required by many micromechanics processes—especially those that must achieve high Q. Thus, compromises in either the circuits process or the micromechanics process have been necessary, undermining the overall modularity of the process. The MICS process (Fig. 11 [11]), which used tungsten metallization instead of aluminum to withstand the high temperatures used in a following polysilicon surface micromachining module, is a good example of a post-circuits process that compromises its metallization technology. More recent renditions of this process have now been introduced that retain aluminum metallization, while substituting lower temperature poly-SiGe as the structural material, with very little (if any) reduction in micromechanical performance [12].

There are number of other processes that can to some extent be placed in more than one of the above categories. These include front bulk-micromachining processes using anisotropic wet etchants [13] and other processes that slightly alter conventional CMOS processes [14]. In addition, bonding processes, in which circuits and µmechanics are merged by bonding one onto the wafer of the other, are

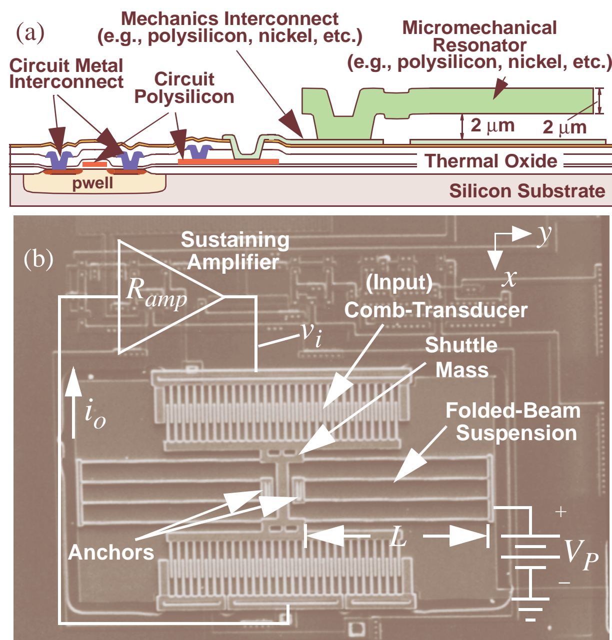

Fig. 11: (a) Cross-section of the MICS process [11]. (b) Overhead-view of a fully integrated micromechanical resonator oscillator fabricated using MICS [2].

presently undergoing a resurgence [15]. In particular, the advent of more sophisticated aligner-bonder instruments are now making possible much smaller bond pad sizes, which soon may enable wafer-level bonding with bond pad sizes small enough to compete with fully planar processed merging strategies in interface capacitance values. If the bond capacitance can indeed be lowered to this level with acceptable bonding yields, this technology may well be the ultimate in modularity.

From a broader perspective, the integration techniques discussed above are really methods for achieving low capacitance packaging of microelectromechanical systems. As mentioned in Section II, another level of packaging is required to attain high Q vibrating μmechanical resonators: vacuum encapsulation. Although the requirement for vacuum is unique to vibrating μmechanical resonators, the requirement for encapsulation is nearly universal for all of the μmechanical devices discussed in this paper, and for virtually all micromechanical devices in general. In particular, some protection from the environment is necessary, if only to prevent contamination by particles (or even by molecules), or to isolate the device from electric fields or feedthrough currents. Needless to say, wafer-level encapsulation is presently the subject of intense research [16].

V. Conclusions

Micromechanical circuits attained via MEMS technologies have been described that can potentially play a key role in removing the board-level packaging requirements that currently constrain the size of communication transceivers. In addition, by combining the strengths of integrated μmechanical and transistor circuits, using both in massive quantities, previously unachievable functions become possible that may soon enable alternative transceiver architectures with substantial performance gains, especially from a power perspective. However, before generating too much enthusiasm, it should be understood that RF MEMS technology is still in its infancy, and much research is needed (e.g., on frequency extension, trimming methods, vacuum encapsulation, and much more) before fully-integrated RF MEMS systems can become a reality.

References

[1] C. T.-C. Nguyen, L. P.B. Katehi, and G. M. Rebeiz, "Micromachined devices for wireless communications (invited)," *Proc. IEEE,* vol. 86, no. 8, pp. 1756-1768, Aug. 1998.

[2] C. T.-C. Nguyen and R. T. Howe, "An integrated CMOS micromechanical resonator high-Q oscillator," *IEEE J. Solid-State Circuits*, vol. 34, no. 4, pp. 440-445, April 1999.

[3] F. D. Bannon III, J. R. Clark, and C. T.-C. Nguyen, "High frequency micromechanical filters," to be published in the April 2000 issue of *IEEE J. Solid-State Circuits* in April 1999.

[4] K. Wang, Y. Yu, A.-C. Wong, and C. T.-C. Nguyen, "VHF free-free beam high-Q micromechanical resonators," *Technical Digest,* 12th Int. IEEE MEMS Conference, Orlando, Florida, Jan. 17-21, 1999, pp. 453-458.

[5] A.-C. Wong, J. R. Clark, and C. T.-C. Nguyen, "Anneal-activated, tunable, 68MHz micromechanical filters" *Digest of Technical Papers*, 10th Int. Conf. on Solid-State Sensors and Actuators, Sendai, Japan, June 7-10, 1999, pp. 1390-1393.

[6] A.-C. Wong, H. Ding, and C. T.-C. Nguyen, "Micromechanical mixer+filters," *Technical Digest,* IEEE IEDM, San Francisco, California, Dec. 6-9, 1998, pp. 471-474.

[7] C. T.-C. Nguyen, "Frequency-selective MEMS for miniaturized low-power communication devices," *IEEE Trans. Microwave Theory Tech*., vol. 47, no. 8, pp. 1486-1503, Aug. 1999.

[8] C. Goldsmith, J. Randall, S. Eshelman, T. H. Lin, D. Denniston, S. Chen and B. Norvell, "Characteristics of micromachined switches at microwave frequencies," IEEE MTT-S Digest, pp. 1141-1144, June, 1996.

[9] T. A. Core, W. K. Tsang, S. J. Sherman, "Fabrication technology for an integrated surface-micromachined sensor," *Solid State Technology*, pp. 39-47, Oct. 1993.

[10] J. H. Smith, S. Montague, J. J. Sniegowski, J. R. Murray, *et al*., "Embedded micromechanical devices for the monolithic integration of MEMS with CMOS," *Proceedings*, IEEE IEDM, Washington, D.C., Dec. 10-13, 1995, pp. 609-612.

[11] J. M. Bustillo, G. K. Fedder, C. T.-C. Nguyen, and R. T. Howe, "Process technology for the modular integration of CMOS and polysilicon microstructures," *Microsystem Technologies*, **1** (1994), pp. 30-41.

[12] A. E. Franke, D. Bilic, D. T. Chang, P. T. Jones, T.-J. King, R. T. Howe, and G. C. Johnson, "Post-CMOS integration of germanium microstructures," *Technical Digest*, 12th Int. IEEE MEMS Conf., Orlando, FA, Jan. 17-21, 1999, pp. 630-637.

[13] H. Baltes, O. Paul, and O. Brand, "Micromachined thermally based CMOS microsensors," *Proc. IEEE*, vol. 86, no. 8, pp. 1660-1678, Aug. 1998.

[14] G. K. Fedder, S. Santhanam, M. L. Reed, S. C. Eagle, D. F. Guillou, M. S.-C. Lu, and L. R. Carley, "Laminated high-aspect-ratio microstructures in a conventional CMOS process," *Sensors and Actuators*, vol. A57, no. 2, pp. 103-110, March 1997.

[15] A. Singh, D. A. Horsley, M. B. Cohn, A. P. Pisano, and R. T. Howe, "Batch transfer of microstructures using flip-chip solder bonding," *J. Microelectromech. Syst*., vol. 8, no. 1, pp. 27-33, March 1999.

[16] K. S. Lebouitz, A. Mazaheri, R. T. Howe, and A. P. Pisano, "Vacuum encapsulation of resonant devices using permeable polysilicon," *Technical Digest,* 12th Int. IEEE MEMS Conf., Orlando, Florida, Jan. 17-21, 1999, pp. 470-475.